Investigation on the fan-shape distribution of surface roughness on diamond-turned single crystal germanium*

SHI Guoquan (史国权), CAI Yongxiang (蔡永祥), YU Junyi (于骏一),
(Department of Mechanical Engineering, Jilin University of Technology, Changchun 130025, China)

MA Wensheng (马文生), HAN Rongjiu (韩荣久) and HUANG Wei (黄 巍)
(State Key Laboratory of Applied Optics, Changchun 130022, China)

Received June 19, 1995

Abstract The cutting force distribution models of diamond-turned single crystal germanium are established. The formation mechanisms of the fan-shape distribution of surface roughness on diamond-turned surface of single crystal germanium are investigated. The homogeneous smooth surface of roughness value $R_a = 0.07 - 0.009\ \mu m$ is obtained by fly cutting of the single crystal germanium, which was performed in the most favourable cutting direction.

Keywords: single crystal germanium, diamond turning, surface roughness, fan-shape distribution.

In ultraprecision cutting, since the depth of cut is usually less than the average grain size of polycrystalline material, the cutting is performed actually within a grain, so many researchers pay close attention to the research on the influence of material anisotropy on the cutting process and the machined surface quality[1-6]. The fan-shape distribution characteristics of surface roughness is one of the projects to be investigated.

Single crystal germanium is one of the functional materials used in infrared optics and reflective optics. It also found wide applications in electronical and astronavigational industry. The single crystal germanium is an anisotropical material, possessing crystal structure the same as natural diamond[1]. The fan-shape distribution of surface roughness appears when the cutting direction varies successively relative to the turned crystal in face turning (see fig. 1). Fig. 1. is the external photograph of the turned surface of single crystal germanium, where the black regions are "clear regions" (fig. 1(a)), and the white ones are the "cloudy regions" (fig. 1(b)). The surface roughness values of some fan-shape regions are small; the surface presents clear appearance. The surface roughness values of some other fan-shape regions are big; the surface presents a cloudy appearance. The pits and cracks remain on the machined surface because of microfractures formed in cutting process. The formation machanism of the fan-shape distribution of surface roughness on diamond-turning single crystal germanium needs further investigation, and a new cutting method for machining

* Project supported by the Scientific Research Foundation of State Key Laboratory of Applied Optics

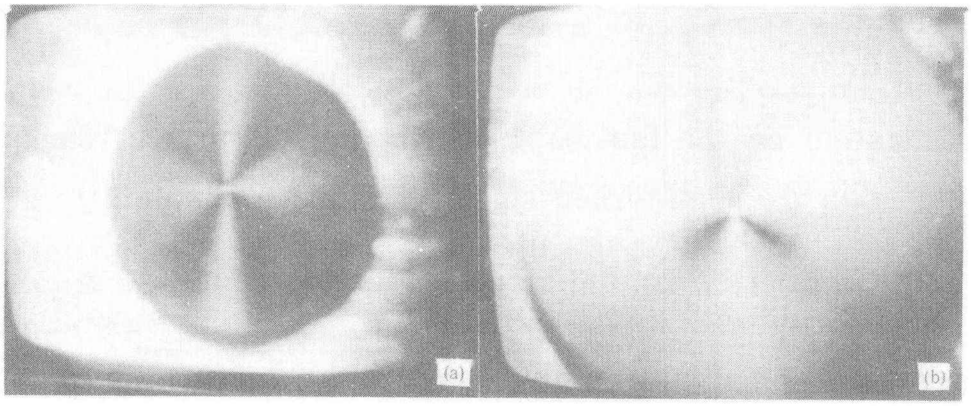

Fig. 1. External photographs of the turned surfaces of single crystal germanium.

an even smoother surface on the anisotropic materials needs to be found.

1 Formation mechanism of the fan-shape distribution of surface roughness on diamond-turning single crystal germanium

The cleavage and slip planes of single crystal germanium are on the (111) planes.[1] The angle between the resultant cutting force and cleavage plane varies successively during diamond face turning single crystal germanium. The normal cutting force component and the tangential cutting force component on (111) plane also vary successively. So the chip removal mode is determined by the orientation of the machined plane relative to the cutting force direction. To recognize the formation mechanism of the fan-shape characteristic of surface roughness during cutting single crystal germanium, the normal cutting force component and tangential cutting force component on the (111) plane should be analyzed first. Fig. 2 shows the schematic of octahedron structure of single crystal germanium, where the angle α between plane (100) (□ *ABCD*) and plane (111) (△ *BCE*) is 54.74°; the angle β between plane (110) (□ *HFIE*) and plane (111) (△ *CDE*) is 35.26°; the angle γ between plane (111) and plane (111) (the outer surface of the octahedron) is 109.48°. The varying regularity of the normal and tangential cutting force components during turning different crystal planes are to be

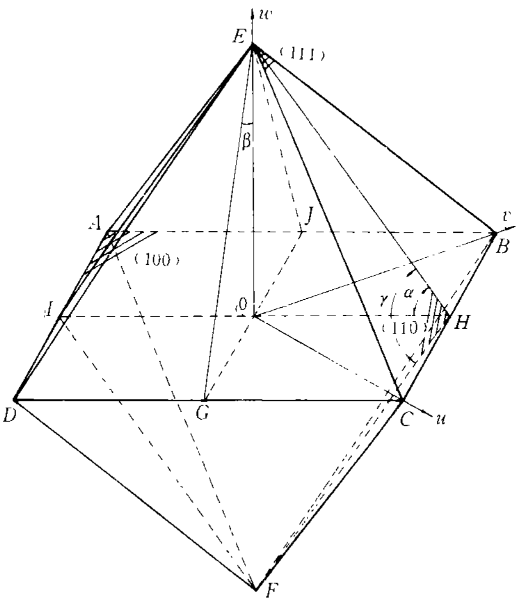

Fig. 2. Structure schematic of single crystal germanium of octahedron structure.

discussed as follows.

1.1 Turning crystal plane (100)

During turning plane (100), the positional relationship between cutting force and plane (111) is shown in fig. 3. Suppose that the base crystal orientation is $\langle 0\bar{1}1\rangle$; the cutting direction of point M is $\langle u\ v\ w\rangle$; the angle between $\langle u\ v\ w\rangle$ and $\langle 0\bar{1}1\rangle$ is θ, which is positive in counter clockwise direction. F_z is the principal cutting force; F_y the thrust force and F_x is the feed force. F_x', F_y' and F_z' are the resultant cutting forces of the components F_x, F_y and F_z which act on crystal plane (100). F_x', F_y' and F_z' are respectively in $\langle 0\bar{1}\bar{1}\rangle$, $\langle 100\rangle$ and $\langle 0\bar{1}1\rangle$ as follows:

$$F_x' = F_z\sin\theta + F_x\cos\theta \qquad \langle 0\bar{1}\bar{1}\rangle,$$

$$F_y' = F_y \qquad \langle 100\rangle,$$

$$F_z' = F_z\cos\theta - F_z\sin\theta \qquad \langle 0\bar{1}1\rangle.$$

Let F_x', F_y' and F_z' be resolved into cleavage plane (111) ($\triangle BCE$) in crystal orientations $\langle \bar{2}1\bar{1}\rangle$, $\langle 111\rangle$ and $\langle 0\bar{1}1\rangle$. Then we have

$$F_z'' = F_x'\cos\alpha + F_y'\cos(90^\circ - \alpha) = (F_z\sin\theta + F_x\cos\theta)\cos\alpha + F_y\sin\alpha \qquad \langle \bar{2}1\bar{1}\rangle,$$

$$F_y'' = F_y'\sin(90^\circ - \alpha) - F_x'\sin\alpha = F_y\cos\alpha - (F_z\sin\theta + F_x\cos\theta)\sin\alpha \qquad \langle 111\rangle,$$

$$F_z'' = F_z\cos\theta - F_x\sin\theta \qquad \langle 0\bar{1}1\rangle.$$

Define K as the ratio of the normal cutting force component F_y'' to the tangential cutting force component (resultant cutting force of F_x'' and F_z'')

$$K = \frac{F_y\cos\alpha - (F_z\sin\theta + F_x\cos\theta)\sin\alpha}{\{(F_z\cos\theta - F_x\sin\theta)^2 + [(F_z\sin\theta + F_x\cos\theta)\cos\alpha + F_y\sin\alpha]^2\}^{1/2}}.$$

It is derived finally that

$$K = \left\{\frac{F_x^2 + F_y^2 + F_z^2}{F_z|\cos\theta| - F_x|\sin\theta|)^2 + (F_z|\sin\theta| + F_x|\cos\theta|)^2/3 + 2\sqrt{2}F_y(F_z|\sin\theta| + F_x|\cos\theta|)/3 + 2F_y^2/3} - 1\right\}^{1/2}. \qquad (1)$$

1.2 Turning crystal plane (110)

During turning plane (110), the positional relationship between cutting force and plane (111) ($\triangle BCE$) is shown in fig. 4. By making the same analysis as above, the cutting force components acting on the crystal plane (110) are as follows:

$$F_x' = F_z\sin\theta + F_x\cos\theta \qquad \langle 001\rangle,$$

$$F_y' = F_y \qquad \langle \bar{1}\bar{1}0\rangle,$$

$$F_z' = F_z\cos\theta - F_x\sin\theta \qquad \langle \bar{1}10\rangle.$$

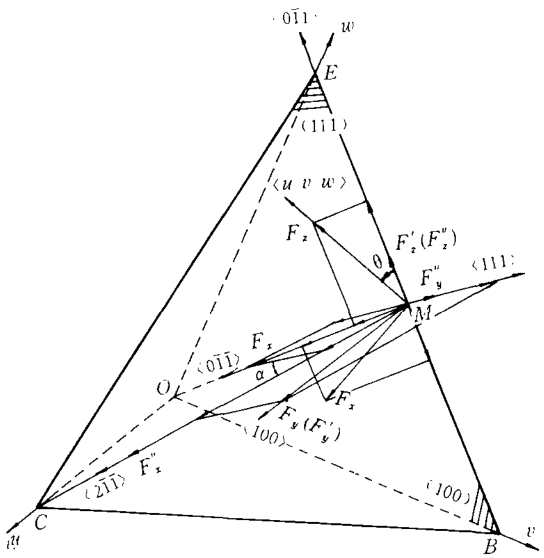

Fig. 3. Positional relationship between cutting force and cleavage plane (111) during turning crystal plane (100). (symbols in figs. 3—5 are the same as those in fig. 2)

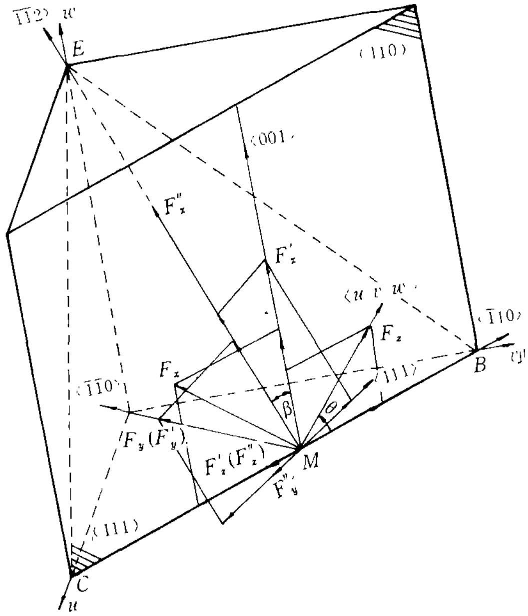

Fig. 4. Positional relationship between cutting force and cleavage plane (111) during turning crystal plane (110).

The cutting force components acting on the crystal plane (111) can be written as

$$F_x'' = (F_z\sin\theta + F_x\cos\theta)\cos\beta + F_y\sin\beta \qquad \langle\bar{1}\,\bar{1}2\rangle,$$

$$F_y'' = (F_z\cos\theta + F_x\cos\theta)\sin\beta - F_y\cos\beta \qquad \langle 111\rangle,$$

$$F_z'' = F_z\cos\theta - F_x\sin\theta \qquad \langle\bar{1}10\rangle.$$

As a result, we have

$$K=\left\{\frac{F_x^2+F_y^2+F_z^2}{(F_z|\cos\theta|-F_x|\sin\theta|)^2+\ 2(F_z|\sin\theta|+F_x|\cos\theta|)^2/3+2\sqrt{2}\,F_y(F_z|\sin\theta|+F_x|\cos\theta|)/3+F_y^2/3}-1\right\}^{1/2}. \tag{2}$$

1.3 Turning crystal plane (111)

The positional relationship between cutting force and plane (111) is shown in fig. 5. By making the same analyses as above, the cutting force components acting on the crystal plane $(\bar{1}11)$ ($\triangle ABE$) are obtained:

$$F_x' = F_z\sin\theta + F_x\cos\theta \qquad \langle\overline{2}\,\overline{1}\,\overline{1}\rangle,$$

$$F_y' = F_y \qquad \langle 1\overline{1}\,\overline{1}\rangle,$$

$$F_z' = F_z\cos\theta + F_x\sin\theta \qquad \langle 0\overline{1}\,1\rangle.$$

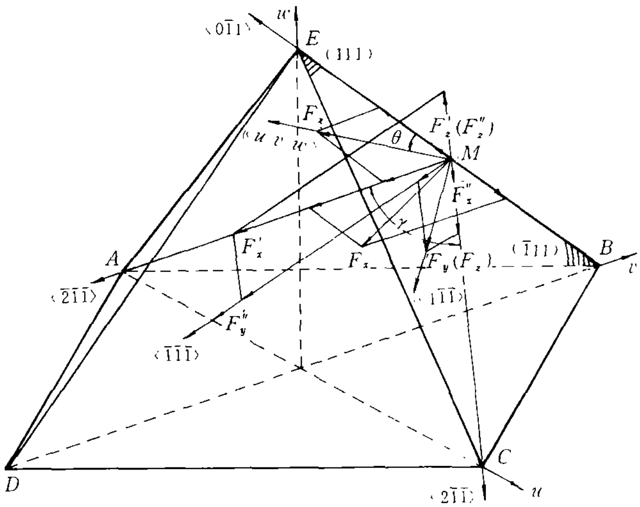

Fig. 5. Positional relationship between cutting force and cleavage plane (111) during turning crystal plane ($\bar{1}11$)

The cutting force components acting on the cleavage plane (111) ($\triangle BCE$) can be written as

$$F_x'' = F_y\cos(\gamma-\pi/2) - (F_z\sin\theta + F_x\cos\theta)\sin(\gamma-\pi/2) \qquad \langle 2\bar{1}\bar{1}\rangle,$$

$$F_y'' = (F_z\sin\theta + F_x\sin\theta)\cos(\gamma-\pi/2) + F_y\sin(\gamma-\pi/2) \qquad \langle 1\bar{1}\bar{1}\rangle,$$

$$F_z'' = F_z\cos\theta - F_x\sin\theta \qquad \langle 0\bar{1}1\rangle.$$

As a result, we obtain

$$K=\left\{\frac{F_x^2+F_y^2+F_z^2}{F_z|\cos\theta|-F_x|\sin\theta|)^2+2(F_z|\sin\theta|+F_x|\cos\theta|)^2/9+4\sqrt{2}F_y(F_z|\sin\theta|+F_x|\cos\theta|)/9+8F_y^2/9}-1\right\}^{1/2}. \qquad (3)$$

Equations (1)—(3) show that the ratio K is a function of angle θ, which means that during the cutting process, the cutting direction varies successively relative to the cleavage plane, so the ratio K also varies successively. In order to recognize the variation of ratio K, a three-dimensional semiconductor load gauge was used to measure the three cutting force components F_x, F_y and F_z. The cutting conditions are listed in table 1. The measured results are as follows:

for turning crystal plane (110): $F_x=0.75N$, $F_y=1.77N$, $F_z=1.55N$;

for turning crystal plane (111): $F_x=0.036N$, $F_y=1.59N$, $F_z=1.22N$.

The ratio K can be calculated according to eqs. (2) and (3). Fig. 6 shows the variation of the calculated ratio K. The larger the ratio K, the greater the brittle fracture tendency. It can be seen from fig. 6 that during cutting crystal plane (110), when the cutting direction coincides with the orientations $\langle\bar{1}10\rangle$, $\langle 1\bar{1}0\rangle$, $\langle 00\bar{1}\rangle$, and $\langle 001\rangle$, the tendency causing

Table 1 Experimental conditions

Sample	single crystal germanium turned planes (110), (111)
Cutting tool	single point diamond tool rake angle $\gamma_0 = -25^\circ$ relief angle $\alpha_0 = 5^\circ$ nose radius $R = 0.8$ mm
Cutting parameter	spindle speed $n = 1\,000$ r/min feed rate $f = 10\ \mu$m/r depth of cut $a_p = 20\ \mu$m

brittle fracture is most serious, and that during cutting crystal plane (111), when the cutting direction coincides with the crystal orientations $\langle 1\bar{2}1\rangle$, $\langle 11\bar{2}\rangle$ and $\langle \bar{2}11\rangle$, the tendency causing brittle fracture is most serious. When the cutting process is furthered nearby the above orientation, the surface roughness values increase, the pits and cracks remain on turned surface, and consequently form some fan-shape regions which present cloudy appearance. On the other hand, when the cutting process is in progress away from the above orientation, the surface roughness values decrease and there form some fan-shape regions which have clear appearance. It can be seen from the above analyses that there are two dark cloudy regions and two light cloudy regions on turned crystal plane (110), and there are three cloudy regions and three clear regions on turned plane (111).

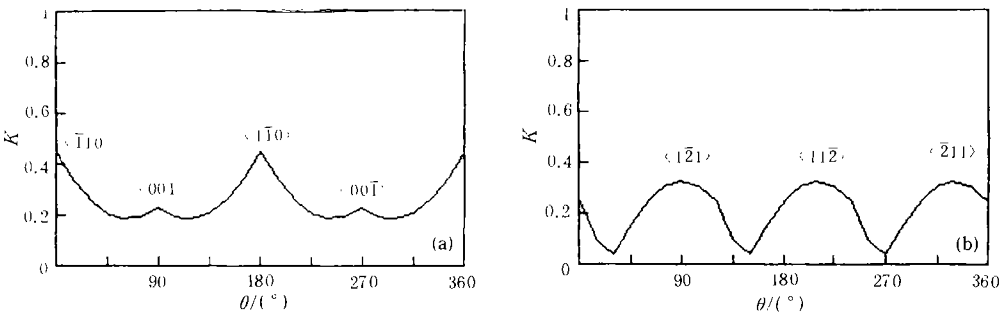

Fig. 6. Variation of ratio K versus angle θ in diamond turning of single crystal germanium. (a) Crystal plane (110); turning crystal plane (111).

2 Experimental verification

In order to verify the varying regularity of surface roughness in diamond-turning single crystal germanium, experiments were performed on an MSG-325 double-axis numerically-controlled diamond lathe produced by Rank Pneumo Co. Ltd. The surface roughness was measured with a Form Talysurf profilemeter. The experimental conditions are listed in table 1.

Figure 7 shows the distribution of surface roughness in a circle of turned surface. It can be known from analyzing the experimental results that the surface roughness is smaller in clear region, but larger in cloudy region. The variation regularity of surface roughness relative to the cutting direction agrees well with that of the theoretical analysis mentioned above.

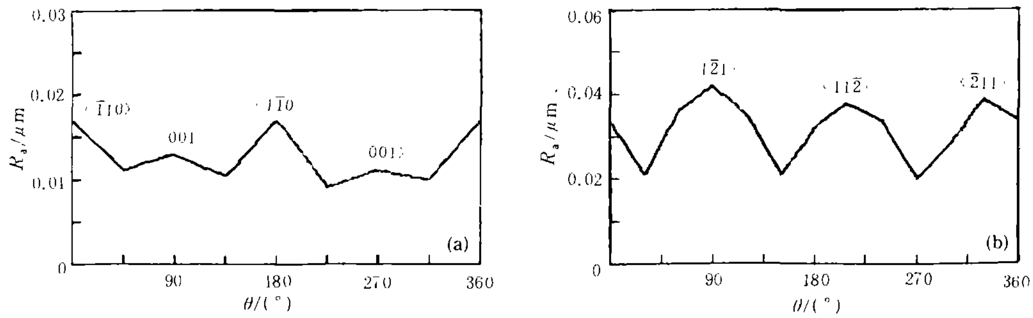

Fig. 7. Distribution of surface roughness measured on turned surface. (a) Turned crystal plane (110); (b) turned crystal plane (111).

3 Fly cutting

Based on the above analysis, the fly cutting method was presented. In fly cutting, the rotating plate was mounted onto the lathe spindle; the workpiece was fixed into the fixture mounted on the slide, and the cutting direction coincided with the direction of the valley value of ratio K. The cutting parameters and diamond tool are the same as those in diamond face-turning crystal plane (110). Fig. 8(a) is the external photograph of machined surface by fly cutting, where the fan-shape regions disappear. Fig. 8(b) gives the surface roughness values in the range of 0.007—0.009 μm measured in one circle of machined surface, which can be used in optical system directly.

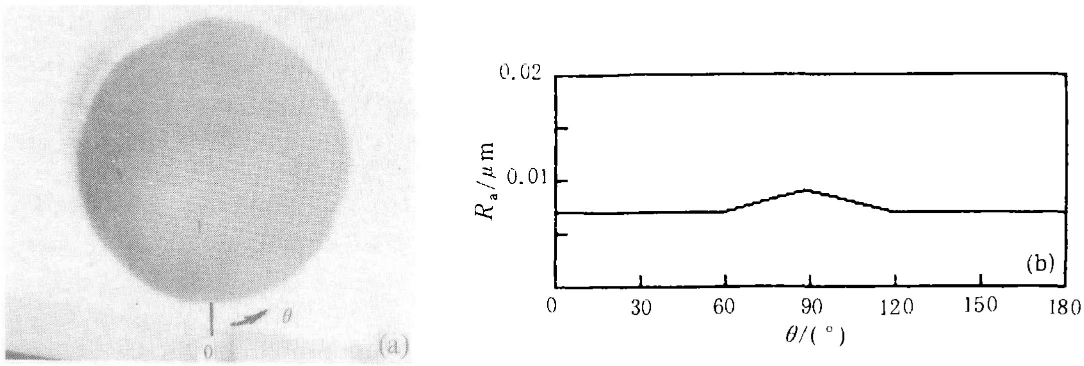

Fig. 8. Experimental results of fly cutting crystal plane (110). (a) External photograph; (b) distribution of surface roughess.

References

1 Nakasuji, T., Kodera, S., Hara, S. *et al.*, Diamond turning of brittle materials for optical components, *Annals. of the CIRP*, 1990, 39(1): 89.

2 Ueda, K., Iwata, K., Chip formation mechanism in single crystal cutting of β-brass, *Annals. of the CIRP*, 1980, 29(1): 41

3 Lee, W. B., Zhou, M., A theoretical analysis of the effect of crystallographic orientation on chip formation in micromachining, *Int. J. Mach. Tools Manufact.*, 1993, 33(3): 439.

4 Yuan, Z. J., Lee, W. B., Yao, Y. X. *et al.*, Effect of crystallographic orientation on cutting forces and surface quality in diamond cutting of single crystal, *Annals. of the CIRP*, 1994, 43(1): 39.

5 Moronuki, N., Liang, Y., Furukawa, Y., Experiments on the effect of material properties on microcutting proccesses, *Precision Engineering*, 1994, 16(2): 124.

6 Blake, P. N., Scattergood, P. O., Ductile-regime machining of germanium and silicon, *J. of the Amerian Ceramic Society*, 1990, 73: 949.